SUPPLEMENTARY MATERIAL FOR

Title: **Discovery and Characterization of Novel Non-substrate and Substrate NAMPT Inhibitors**

Authors: Julie L. Wilsbacher[1,*], Min Cheng[1], Dong Cheng[1], Samuel A. J. Trammell[2,3], Yan Shi[1], Jun Guo[1], Stormy L. Koeniger[1], Peter J. Kovar[1], Yupeng He[1], Sujatha Selvaraju[1], H. Robin Heyman[1], Bryan K. Sorensen[1], Richard F. Clark[1], T. Matthew Hansen[1], Kenton L. Longenecker[1], Diana Raich[1,4], Alla V. Korepanova[1], Steven Cepa[1], Danli L. Towne[1], Vivek C. Abraham[1], Hua Tang[1], Paul L. Richardson[1], Shaun M. McLoughlin[1], Ilaria Badagnani[1], Michael L. Curtin[1], Michael R. Michaelides[1], David Maag[1], F. Greg Buchanan[1], Gary G. Chiang[1, 5], Wenqing Gao[1], Saul H. Rosenberg[1], Charles Brenner[2] and Chris Tse[1]

Author affiliations: [1]AbbVie Inc., 1 North Waukegan Rd., North Chicago, IL 60064, USA

[2]Department of Biochemistry Carver College of Medicine, University of Iowa, Iowa City, IA, USA

[3]Current address: The Novo Nordisk Foundation Center for Basic Metabolic Research, Section for Metabolic Imaging and Liver Metabolism, University of Copenhagen, 2200 Copenhagen, Denmark

[4]Current address: MPI Research, 54943 North Main Street, Mattawan, MI 49071, USA

[5]Current address: eFFECTOR Therapeutics, San Diego, CA 92121, USA

Running title: Novel non-substrate NAMPT inhibitors

SUPPLEMENTARY METHODS

High throughput cellular screen and target identification

An initial high throughput screen was performed to identify compounds that show differential cytotoxicity after ~72 hours of compound treatment in A375 (B-Raf V600E mutant) and PC3 (B-Raf WT) cells. Cytotoxicity was determined using the CellTiter Glo cell viability assay that detects total intracellular ATP (Promega). 450,000 compounds were first tested as mixtures (1 μM each; 10 μM total/well) against A375 cells. Actives were defined as compounds displaying ≥50% growth inhibition and were confirmed by retesting as single compounds at 1 μM. 4092 confirmed active compounds were then tested in dose response in both A375 and PC3 cells, and 63 compounds with IC_{50} values displaying ≥10-fold selectivity toward either A375 or PC3 cells were subsequently screened in a panel of eight cancer cell lines that included four melanoma cell lines (A375, SKMEL28, Malme-3M, and MeWo) and four prostate cancer cell lines (PC3, LNCaP, DU145, and 22RV1). One of the objectives of the screen was to identify novel compounds with unknown mechanisms of action, so all selective compounds were progressed, whether they satisfied the BRAFV600E-selective criterion or not. Compounds were tested in dose response in the 8-cell line panel in a 5-day CellTiter Glo cell viability assay. Hierarchical clustering of the cell line panel IC_{50} values was performed to identify distinct selectivity profiles.

HCT116 cell pellets were lysed in 1% Triton X-100, 150 mM NaCl, and 10 mM HEPES with protease and phosphatase inhibitors for 1 hour then clarified by centrifugation. DMSO or 50 μM or competitor compounds (FK866 or A-933414) were added to 1 mL (17.2 mg) of lysate and incubated overnight. Anti-FLAG M2 affinity resin (100 μl of a 50% slurry) per sample was mixed with 10 μM FLAG-FK866 or 10 μM FLAG-A-933415 and incubated for 2 hours. M2 resin-FLAG complexes were then washed 10 times with lysis buffer and stored overnight. Resins were washed 3 times in lysis buffer and 100 uL of the washed resins were added to each lysate sample: 10 μM FLAG-FK866 was added to lysates treated with DMSO or FK866 as the competitor compound and 10 μM FLAG-A-933415 was added to lysates treated with DMSO or A-933414 as the competitor compound. Targets were captured for 4 hours, then washed and

bound proteins were eluted from the M2 resins with 3xFLAG. Eluates were concentrated and proteins were separated via SDS-PAGE. Sypro stained bands were identified by LC-MS/MS.

NAMPT biochemical assays

Compound dissociation kinetics were evaluated using a TR-FRET binding assay. Complexes were assembled by pre-incubation of 2 μM His-tagged full-length NAMPT, 2.5 mM ATP, 40 μM PRPP and 2 μM compound in TR-FRET buffer. Complexes were pre-incubated at room temperature for 0.5 or 24 hours to allow potential phosphoribosylation of compounds by the enzyme. Complexes were then diluted 500-fold into TR-FRET buffer containing 2.5 mM ATP, 2 nM terbium-conjugated anti-His antibody, with or without 40 μM PRPP. Complexes were incubated at room temperature for 30 minutes to allow antibody binding to reach equilibrium. Complexes were then diluted into a large excess (1 μM final) of an active site probe labeled with Oregon Green-488 and the increase in TR-FRET signal was measured as a function of time. As compound dissociation is rate-limiting under these conditions, observed reaction kinetics are indicative of compound dissociation. Raw data were normalized to both a high control (probe bound to enzyme prior to compound addition) and a low control (no enzyme) and fit with a double exponential.

Protein sample preparation

The full-length DNA encoding the human NAMPT, residues 1 to 491 (GenBank Accession Number NM_005746.2) with the FLAG-tag (DYKDDDDK) introduced at the C-terminus was synthesized and cloned into the pLVX-IRES-puro expression vector. The protein construct NAMPT (1-491)-Flag was transiently expressed in HEK 293-6E cells (NRC-Canada) using a Wave Bioreactor (System 20/50EHT, GE Healthcare) at 25 L scale. NAMPT protein expressed intracellularly was purified using two columns. Briefly, cellular lysate in 50 mM Tris, pH7.5, 200 mM NaCl, 0.1% Triton X-100, 0.5 mM $MgCl_2$, 1 mM NaN_3 supplemented with benzonase (Cat # 1.01697.0001, EMD Millipore Co.) and protease inhibitor cocktail (Cat# 04574834, Roche Diagnostics) was clarified by centrifugation at 12,000 x g for 30 minutes at 4°C, mixed with anti-FLAG M2 affinity resin (A2220, Sigma-Aldrich) and equilibrated in Column buffer: 50 mM TrisHCl, pH 7.5, 200 mM NaCl, 1 mM EDTA, 1 mM NaN_3. The protein sample was incubated with the resin for 1 hour at room temperature and with gentle mixing. The

column was set by gravity flow and washed extensively with the Column buffer. The protein was eluted with several aliquots of 0.1 mg/mL FLAG-peptide (F3290, Sigma). The protein was further purified using a HiPrep Sephacryl S200 26/60 High Resolution SEC column (cat# 17-1195-01, GE Healthcare). The protein in final 50 mM Tris, pH 8.0, 200 mM NaCl, 1 % glycerol (w/v), 5 mM β-mercaptoethanol, 1 mM NaN_3 buffer was concentrated using Amicon Ultra 30K centrifugal concentrators (cat#UFCB803024, Millipore) followed by concentrating with Microcon Ultracel YM-30 (cat#42410, Millipore). The protein at 10-13 mg/mL was used for crystallization and X-ray studies.

Compound phosphoribosylation

For enzymatic modification assays, compounds at final concentrations of 1 μM were incubated with 250 nM His-tagged full-length NAMPT, 2.5 mM ATP, 40 μM PRPP and 20 μM NAM for 3 hours, then 20 mM EDTA was added to stop the reactions. Reactions were diluted 1:1 in acetonitrile (ACN), and LC-MS analysis was performed to measure unmodified compound and phosphoribosylated compound percentages. For cellular assays, compounds at a final concentration of 1 μM were added to 1 million PC3 cells/well in 6 well plates. Cells were then incubated for 24 hours followed by harvest. For harvest cells were washed twice with 2 mL Dulbecco's phosphate buffered saline per well, and 500 μL of cold ACN:water (60%:40%) mixture was added per well. Plates were shaken for 30 minutes, followed by transfer of the supernatant to individual Eppendorf tubes and extraction at 4°C overnight. LC-MS analysis was performed to measure unmodified compound and phosphoribosylated compound concentrations in extracts. Analysis was performed using a Thermo DecaXP ion trap mass spectrometer, with chromatographic separation from a Phenomenex Synergi Hydro RP column (3 x 150 mm) using a 300 μL/min gradient of 2% to 80% organic mobile phase over 4 minutes [organic mobile phase of 1:1 ACN:water with aqueous mobile phase of 20 mM ammonium acetate].

Fraction unbound measurements in plasma

Fraction unbound measurements were performed in CD-1 mouse plasma using HTD96b dialysis blocks (HT Dialysis LLC, Gales Ferry, CT). Compounds were dispensed to the donor side of an HTD96b dialysis apparatus in triplicate at a 1 μM final concentration. An equal volume of phosphate buffer was added to the receiver side. After 4 hours of incubation at 37^{o}C

an aliquot was removed from both donor and receiver sides and quenched with excess amount of organic solvent containing internal standard. Samples were centrifuged and analyzed by LC-MS/MS and standard curves were utilized to quantitate the concentration in both the buffer and plasma samples to extend the detection range for tightly protein bound compounds.

Mouse intravenous and oral pharmacokinetics

Male CD-1 mice, weighing 25-35 g, were obtained from Charles River Laboratories (Wilmington, MA). Intravenously dosed pharmacokinetics (PK) studies were conducted using isoflurane anesthetized mice (n=3 animals). The vehicle for intravenous (IV) route was composed of 2.5% DMSO, 2.5% Tween-80, 25% PEG-400, and 5% dextrose in water (D5W); the vehicle for oral route was comprised of 2.5% Ethanol, 5% Tween-80, 25% PEG-400, and hydroxyproyl methyl cellulose (HPMC). The IV dose was 3 mg/kg, while the oral dose was 10 mg/kg. Sequential blood samples were obtained from a tail vein of each animal over an 8 hour period after dosing. Plasma was separated by centrifugation and stored frozen until analysis. Compounds were selectively extracted from plasma using protein precipitation with acetonitrile containing internal standards. Compound concentrations were determined using reverse phase chromatography by LC-MS/MS in positive ion mode. The concentration data were then analyzed by multi-exponential curve fitting using WinNonlin (Pharsight Corporation, Cary, NC). The area under the concentration-time curve from 0 to t hours after dosing (AUC_{0-t}, t = time of the last measurable plasma concentration) was calculated using the linear trapezoidal rule for the concentration-time profiles. The residual area extrapolated to infinity, determined as the final measured plasma concentration divided by the terminal elimination rate constant, was added to AUC_{0-t} to produce the total area under the curve ($AUC_{0-\infty}$). The apparent total plasma clearance (CL_p) was calculated by dividing the administered dose by the $AUC_{0-\infty}$. Bioavailability (F) was calculated as the dose-normalized $AUC_{0-\infty}$ ($AUC_{0-\infty}/D$) from the oral dose divided by the corresponding dose normalized $AUC_{0-\infty}$ from intravenous dosing assuming linear pharmacokinetics. The *in vivo* unbound mouse intrinsic clearance ($CL_{int,u}$ in L/h/kg) was calculated (1) using the well-stirred model, where CL_p is the total mouse plasma clearance, Q_h is the mouse liver blood flow (5.2 L/h/kg), and f_{up} is the fraction unbound in mouse plasma.

$$CL_{int,u} = (Q_h * CL_p)/(f_{up} * (Q_h - CL_p))$$

SUPPLEMENTARY REFERENCES

1. Heinle L, Peterkin V, de Morais SM, Jenkins GJ, Badagnani I. A High Throughput, 384-Well, Semi-Automated, Hepatocyte Intrinsic Clearance Assay for Screening New Molecular Entities in Drug Discovery. Comb Chem High Throughput Screen **2015**;18(5):442-52.

SUPPLEMENTARY TABLES

Table S1. NAMPT crystal structure data and refinement statistics

X-ray diffraction data	+A-1293201	+A-1326133
Space group	$P2_1$	$P2_1$
Unit cell	61, 107, 183 β=96	61, 107, 83 β=97
Resolution	1.89	1.73
Observations	277,495	358,057
Unique	74,091	109,253
Completeness (%)	87.6	97.9
Mean diffraction signal (I/σ)	12	15
R_{merge} (%)	8.1	5.2
Model refinement		
Reflections (work/free)	70138/3689	105,964/5439
R_{factor} (work/free %)	19.2/22.0	19.3/23.9
Mean B value	26	28
RMSD ideal bond length (Å)	0.01	0.01
RMSD ideal bond angles (°)	1.08	1.04

Table S2. NAMPT inhibitor biochemical and cellular properties

Series	Compound	X	Structure	Enzyme activity IC_{50} (nM)	PC3 viability IC_{50} (nM)	PC3+NMN viability IC_{50} (nM)	HCT116 viability IC_{50} (nM)	H1975 viability IC_{50} (nM)
FK866	FK866	N	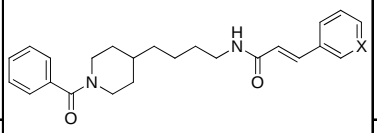	62	5.7	>10,000	1.0	24
FK866	FK866 analog	CH		ND	>10,000	ND	ND	ND
Aza	A-1267211	N	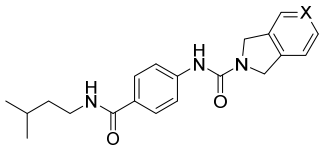	91	8.4	>10,000	6.1	ND
Iso	A-933414	CH		55	38	>10,000	ND	ND
Aza	A-1331597	N	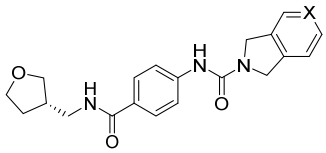	107	41.8	>10,000	32.4	1289
Iso	A-1293201	CH		83	56	>10,000	19	941
Aza	A-1326133	N	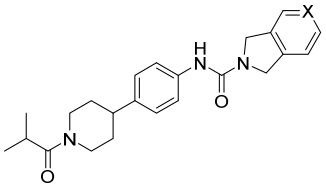	112	1.9	>10,000	0.6	9.8
Iso	A-1292945	CH		98	18	>10,000	7.7	98
Aza	A-1307138	N	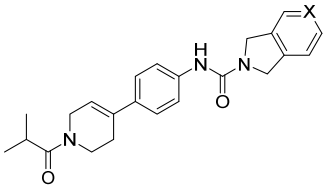	129	2.0	>10,000	0.7	ND

ND: not determined

Table S3. NAMPT inhibitor pharmacokinetics data

Mouse PK parameters	***A-1307138***	***A-1326133***	***A-1293201***
$CL_{int,u}$ (L/hr/kg)	29	17	6.6
CL_p (L/hr/kg)	1.7	2.2	0.78
F (%)	46	81	75
$f_{u,p}$	0.087	0.23	0.14

$CL_{int,u}$: *in vivo* unbound intrinsic clearance, CL_p: total plasma clearance, F: oral bioavailability, $f_{u,p}$: fraction unbound in plasma.

Table S4. Structures and PC3 viability IC_{50} data for isoindoline/azaisoindoline pairs in Figure 2.
See excel file

SUPPLEMENTARY FIGURES

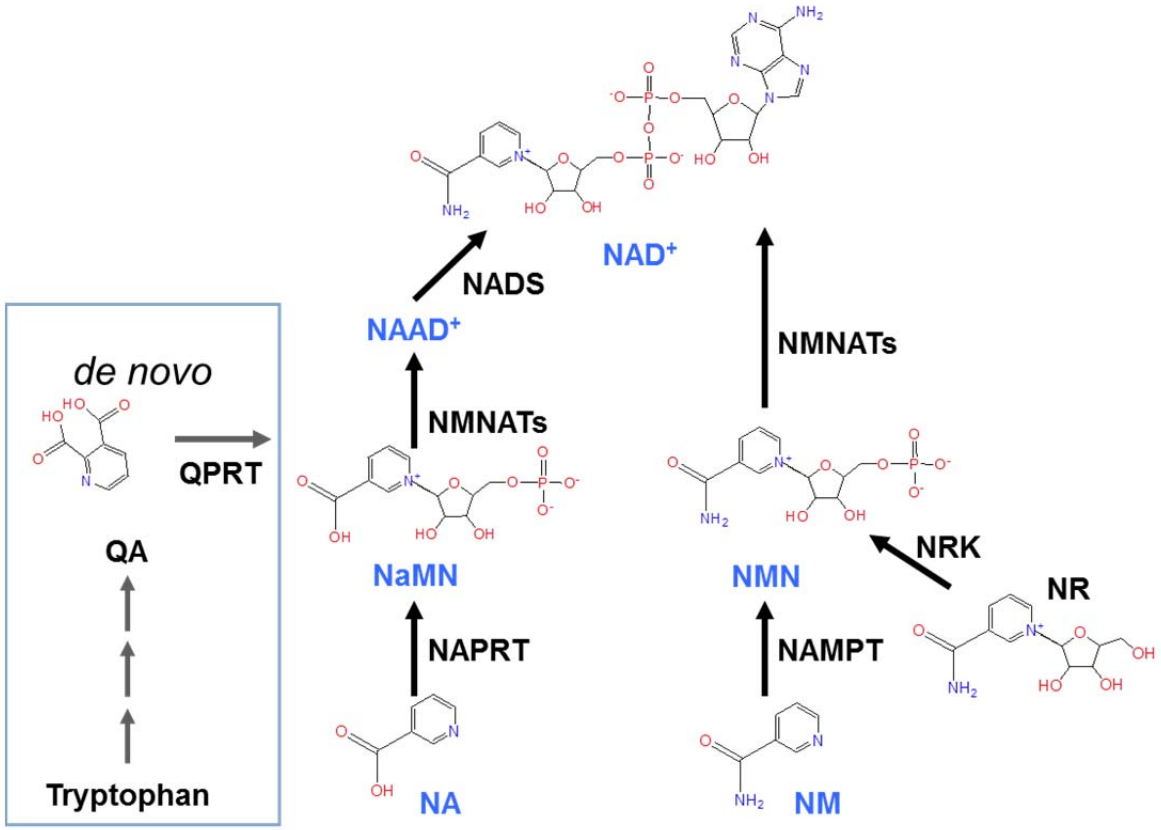

Supplementary figure 1. The human NAD+ biosynthetic pathway. The de novo pathway utilizes the amino acid tryptophan as a substrate to synthesize, through a series of enzymatic steps, quinolinic acid (QA), which is further converted to NAD^+. The primary mechanism of NAD^+ salvage in humans is catalyzed by NAMPT, an enzyme that phosphoribosylates NAM yielding nicotinamide mononucleotide (NMN), which is subsequently adenylated to NAD^+ by nicotinamide mononucleotide adenylyltransferases (NMNAT1-3). NMN can also be formed by phosphorylation of nicotinamide riboside (NR) by nicotinamide riboside kinases (NRKs). Additionally, NAD^+ is synthesized through phosphoribosylation of nicotinic acid (NA) by nicotinic acid phosphoribosyltransferase (NAPRT) to form nicotinic acid mononucleotide (NaMN), which is then adenylated to nicotinic acid adenine dinucleotide ($NAAD^+$) by NMNATs, and finally converted to NAD^+ by NAD^+ synthetase (NADS)-mediated amidation.

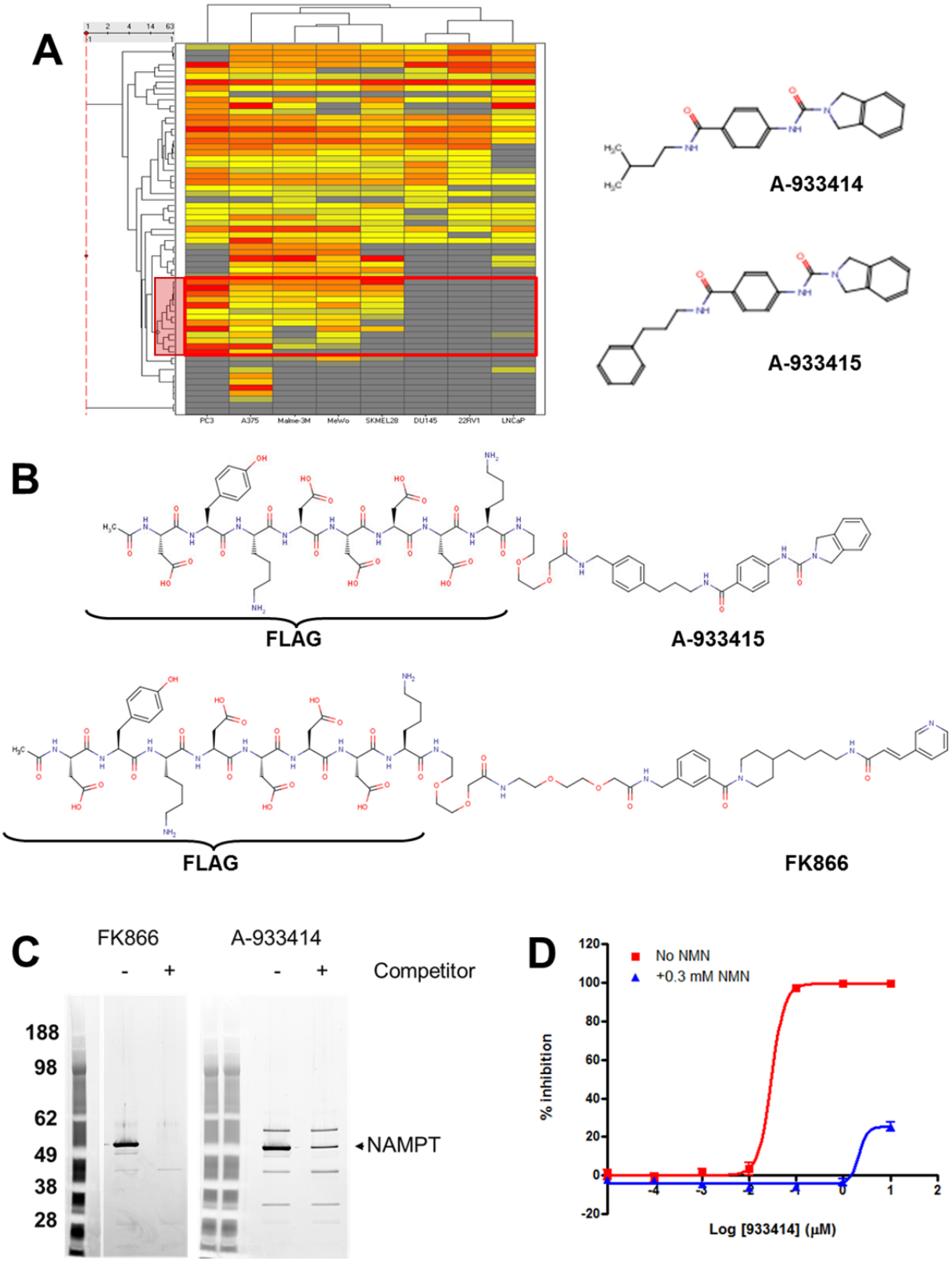

Supplementary figure 2.

Supplementary figure 2. Potent, nicotinamide-competitive, non-substrate inhibitors of NAMPT were identified in a cellular high throughput screen. (A) Top: A cellular screen yielded a set of 63 compounds with highly differential activity across a panel of eight cancer cell lines. A hit cluster comprising compounds structurally similar to and distinct from FK866 was identified (boxed in red). Right: Structures of A-933414 and A-933415, which were used for further characterization. (B) Structures of A-933415-FLAG and FK866 FLAG affinity capture reagents. (C) Inhibitor affinity capture using FK866 –FLAG (left) or A-933415-FLAG (right) followed by SDS-PAGE and Sypro staining revealed a major protein migrating at ~55 kDa, subsequently determined to be NAMPT by LC-MS/MS. Note, the binding of NAMPT to the probe was blocked by 50 μM free competitor compound, FK866 (left) and A-933414 (right). (D) The addition of 0.3 mM NMN to the cell culture medium rescues PC3 cell viability after treatment with A-933414 in a 5-day cell viability assay. Data are the mean ± SEM from 8 independent experiments for no NMN and 2 independent experiments for + 0.3 mM NMN.

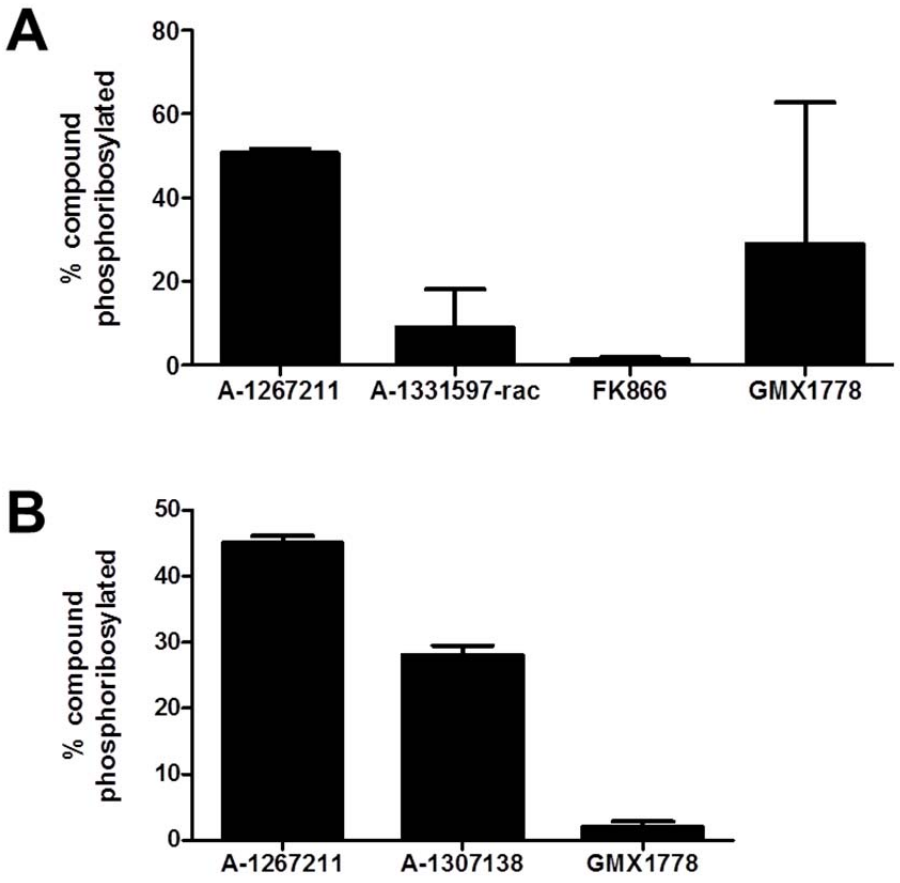

Supplementary figure 3. Phosphoribosylation of azaisoindoline NAMPT inhibitors. (A) 1 μM FK866, GMX1778, A-1267211, or the racemic mixture of A-1331597 (A-1331597-rac) were incubated with NAMPT in enzyme assays and % phosphoribosylation was determined by LC-MS. (B) 1 μM A-1267211, A-1307138, or GMX1778 were added to PC3 cells, which were then incubated for 24 hours followed by harvest. LC-MS analysis was performed to determine % phosphoribosylated compound. Data for both panels are the mean ± SD for duplicate samples and are representative of 1-3 independent experiments.

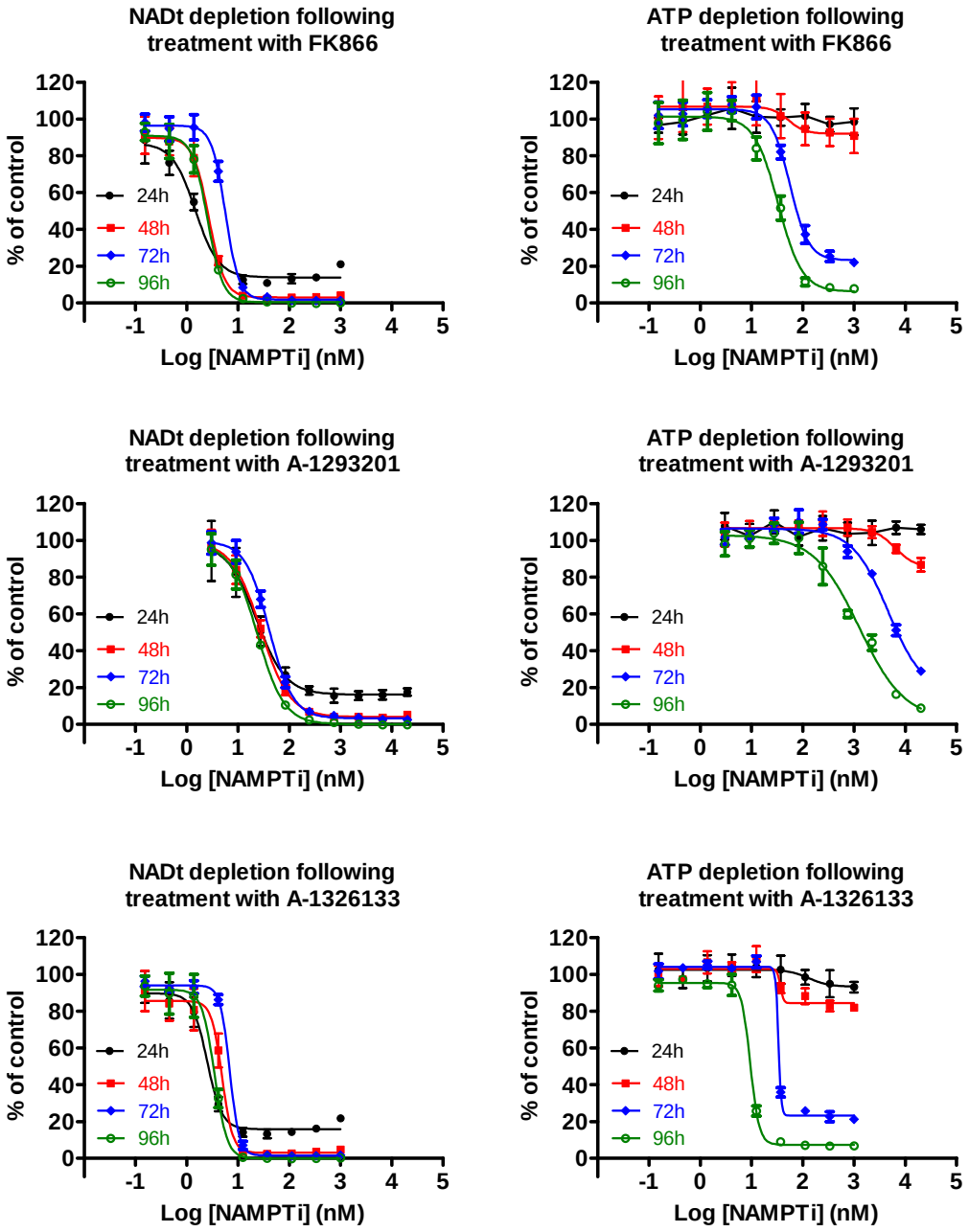

Supplementary figure 4. NADt and ATP depletion in NCI-H1975 cells following FK866, A-1293201 and A-1326133 treatment. Kinetics of NAMPT inhibition in NCI-H1975 cells. Cells were incubated with the indicated concentrations of FK866 (top), A-1293201 (middle) or A-1326133 (bottom) for 24, 48, 72, or 96 hours. NADt and ATP levels were assessed at each time point. Treatment with all compounds resulted in maximal NADt depletion within 48 hours and maximal ATP depletion within 96 hours. Data are the mean ± SD of triplicate samples and are representative of at least 2 independent experiments.

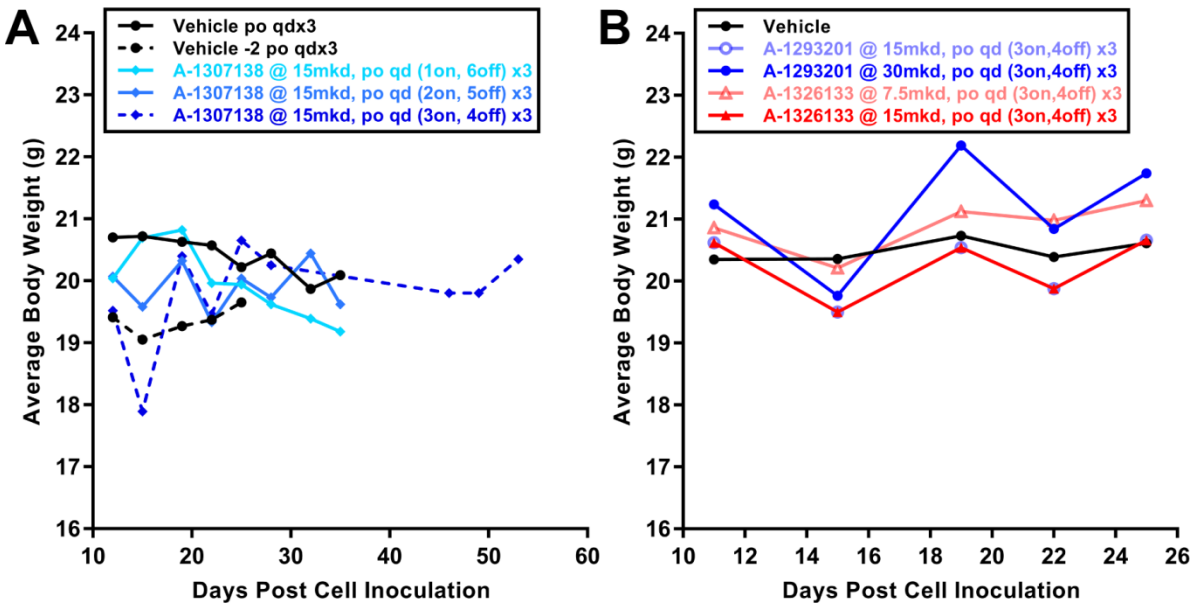

Supplementary Figure 5. Body weight graphs for HCT116 xenograft efficacy studies. (A) Body weight plots for mice bearing HCT116 xenografts and dosed orally (po) once a day (qd) with A-1307138 on different schedules. Body weight curves from two separate experiments are graphed together and curves for each study are designated by solid vs. dashed line. (B) Body weight plots for mice bearing HCT116 xenografts and treated with A-1326133 and A-1293201 at the indicated doses on a po qd (3on,4off) x3 schedule. Body weights are the average for 10 mice/treatment weighed as a group.

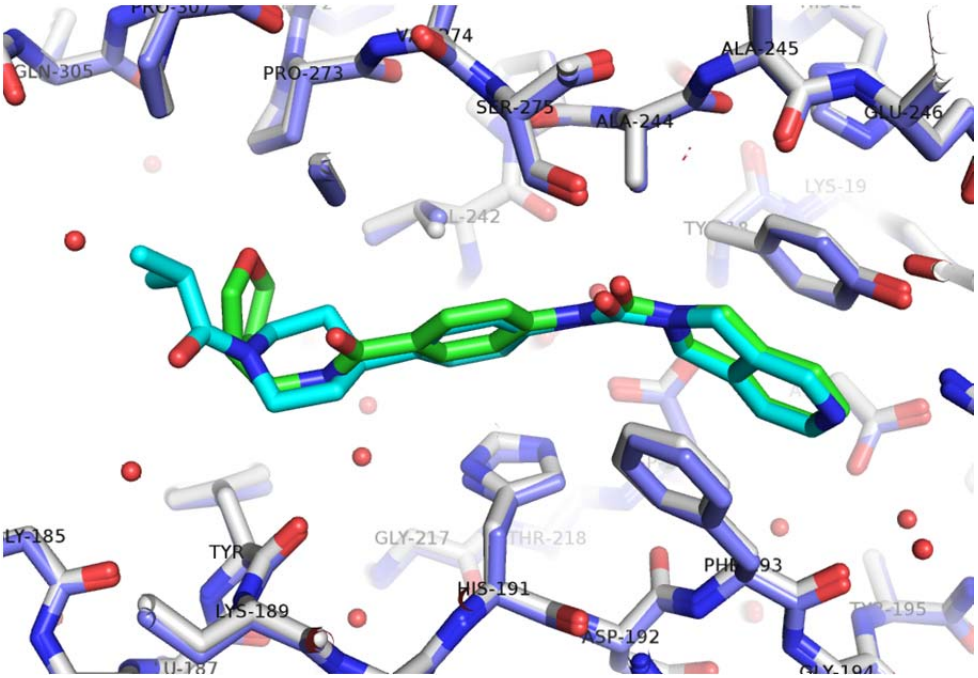

Supplementary figure 6. Overlaid crystal structures of NAMPT complexes with A-1293201 (green, protein gray) and A-1326133 (cyan, protein dark blue).

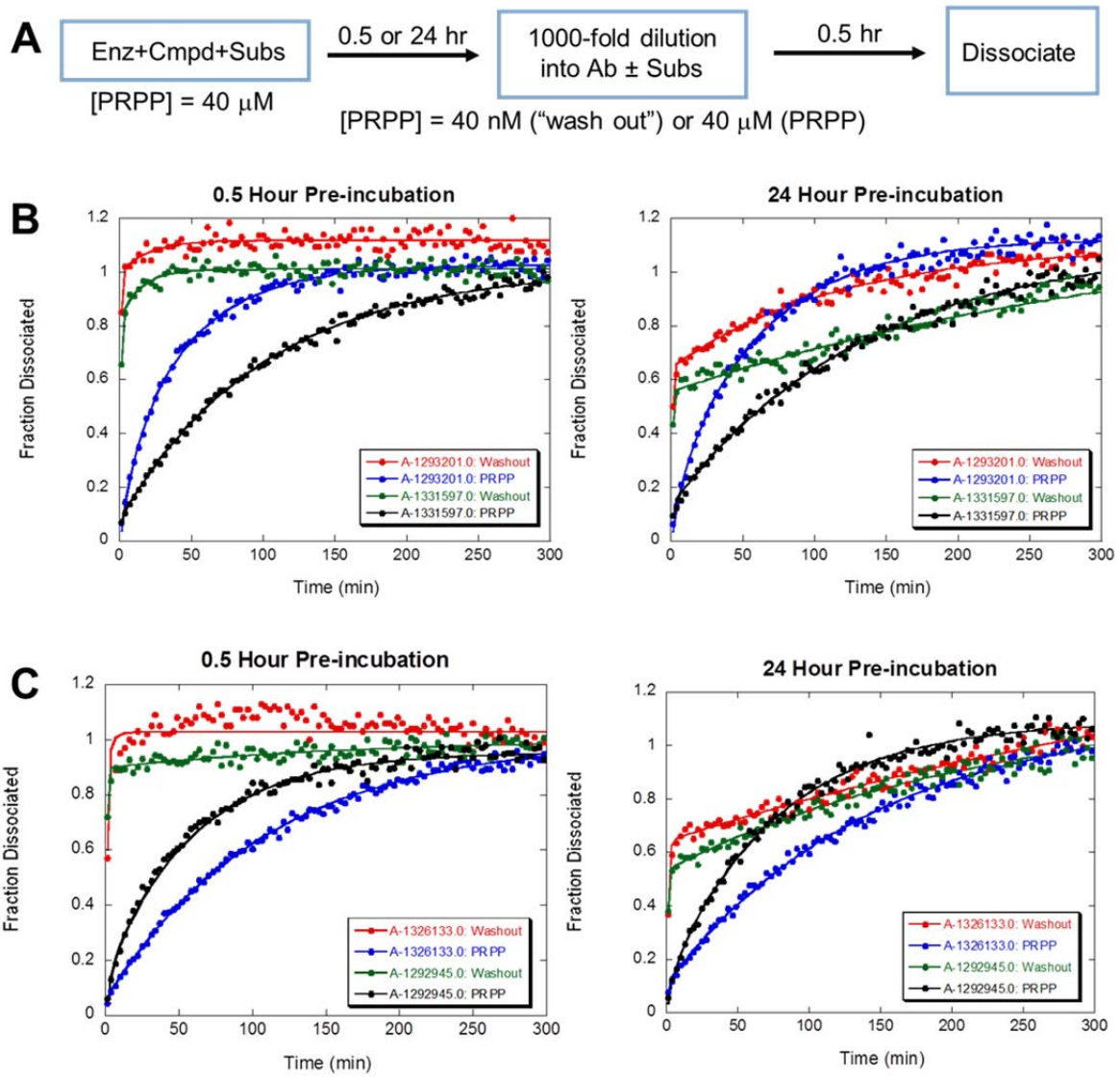

Supplementary figure 7. Residence time of A-1293201 / A-1331597 and A-1326133 / A-1292945 on NAMPT protein. (A) Design of TR-FRET assay used to measure residence time for NAMPT inhibitors. (B) Dissociation curves for A-1293201 and A-1331597 following washout after a 30 minute (left) or 24 hour (right) preincubation of NAMPT enzyme with compounds and PRPP. (C) Dissociation curves for A-1326133 and A-1292945 following washout after a 30 minute (left) or 24 hour (right) preincubation of NAMPT enzyme with compounds and PRPP.